Hue University Journal of Science: Natural Science
Vol. 132, No. 1D, 35–42, 2023

pISSN 1859-1388
eISSN 2615-9678

Effects of Sb on structure, micro structure and electrical characteristics of Sb-modified $(K_{0.41}Na_{0.59})NbO_3$ ceramics

Le Tran Uyen Tu*

University of Sciences, Hue University, 77 Nguyen Hue, Hue, Vietnam

* Correspondence to Le Tran Uyen Tu <tuletranuyen@hueuni.edu.vn>

(*Received: 29 March 2023; Revised: 21 April 2023; Accepted: 28 May 2023*)

Abstract. Lead-free $(Na_{0.59}K_{0.41})(Nb_{1-x}Sb_x)O_3$ ceramic (x = 0 ÷ 0.12) were prepared by the solid phase reaction method. The influence of Sb concentration on the structure, microstructure and electrical properties of the ceramic was studied. Results indicate that the presence of pure perovskite phase was revealed by XRD patterns recorded for the ceramics, which also showed a shift in structure from orthorhombic to mixed rhombohedral and tetragonal with an increase in x value. At x = 0.06, the ceramics express the best microstructure, the particles were tightly packed with an average particle size of 1.76 μm. The $(Na_{0,59}K_{0,41})(Nb_{0,94}Sb_{0,06})O_3$ ceramics have the best dielectric and ferroelectric properties: the ceramic density (ρ) is 4.48 g/cm³ (relative density: 98.7% of the theoretical value); highest dielectric constant at T_C (ε_{max}) of 12031; dielectric constant at RT (ε) of 945; low dielectric loss (tanδ) of 0.15; and high remanent polarization (P_r) of 11,2 μC/cm²; and the reactance field (E_c) of 8.7 kV/cm, and the phase transition temperatures (T_C) of 372 °C, and (T_{O-T}) of 157 °C.

Keywords: Lead free ceramics, Sb-doping, Dielectric response, ferroelectrical properties

1 Introduction

One of the most innovative new materials is ferroelectric ceramics, which is highly significant in a variety of technical fields. Due to lead oxide's toxicity and high vapor pressure during processing, which can pollute the environment, piezoceramic systems have been manufactured and primarily used for lead (PZT) based piezoelectric ceramics for many years [1-4]. Consequently, a great deal of basic and applied research has been carried out on lead-free piezoelectric ceramics [5-7]. Among them, (K, Na)NbO_3 (KNN) based piezoelectric ceramics was the most interested because of its strong ferroelectricity and high Curie temperature (about 420 °C) [8, 9], thereby it has become one of the most promising candidates for replacing Pb-based ceramics. By using a template grain growth method, Li *et al.* [10] created textured KNN-based lead-free ceramics in 2018, which showed improved electrical properties like piezoelectric constant (d_{33} ≈ 700 pC/N) and electromechanical coupling factor (k_P ≈ 0.76). Recently, a novel strategy is developed to construct the *R-T* phase boundary by adding an ABO_3-type component, which can tailor T_{R-O} and T_{O-T} to room temperature simultaneously, and is beneficial to establish the *R-T* phase boundary, leading to the improvement of piezoelectric properties in the KNN-based materials [4, 11].

Therefore, the $(K_{0.41}Na_{0.59})(Nb_{1-x}Sb_x)O_3$ combined with Sb element were introduced to stabilize the perovskite structure and form the *R-T* phase boundary in the KNN based ceramics. Our recent study's [12] findings indicate that lead-free $(K_{0.41}Na_{0.59})NbO_3$ ceramics had the best electrical characteristics (ε = 470, k_P = 0.32, k_t = 0.5, d_{33} = 120

pC/N, P_r = 11.6 μC/cm²) were obtained. This study aimed to address the need for practical applications by examining the impact of $(K_{0.41}Na_{0.59})NbO_3$ lead-free.

2 Experimental section

The traditional mixed-oxide process was used to produce lead-free $(K_{0.41}Na_{0.59})(Nb_{1-x}Sb_x)O_3$ (KNNS) ceramics with x = 0.0, 0.03, 0.06, 0.09, and 0.12. To lessen the impact of moisture, K_2CO_3, Na_2CO_3, Sb_2O_3, Ta_2O_5, and Nb_2O_5 (purity 99.9%) were used as the starting materials. K_2CO_3 and Na_2CO_3 powders were dried for two hours at 150 °C in an oven. After that, the powdered samples were weighed and milled for sixteen hours in ethanol. The sample was then calcined for two hours at 850 °C after being dried, pressed, and heated through two cycles of calcination. The calcined powders were then ball-milled for 20 h and compressed into disks (diameter: 12 mm; thickness: 1.5 mm) at a pressure of 1.5 T/cm² and sintered at 1090 °C for 2 h to produce KNNST ceramics.

The XRD (D8 ADVANCE) technique was used to determine the crystal structure of ceramics, and an SEM system (Hitachi S 4800) was used to assess the morphology and microstructure of the samples. The Archimedes method was used to calculate ceramic density, while the Sawyer-Tower method was used to examine ferroelectric hysteresis loops. The capacitance and dielectric loss of the ceramic samples (RLC HIOKI 3532) were measured using an impedance analyzer.

3 Results and discussion

The changes in the structure of the Sb-doped KNN ceramics containing different amounts of Sb are shown in Fig. 1. As shown in Fig. 1(a), a pure perovskite phase is observed. To study in more detail the phase structure of KNNS ceramics, the XRD patterns investigated at 2θ = 21–24° (Fig. 1(b)) and 2θ = 44–47° (Fig. 1(c)), respectively. The ceramic's structure appears to change from an orthorhombic phase (*O-phase*) with two split peaks at $(202)_O$, lower angle: $(020)_O$; higher angle; $a \approx c > b$) to the tetragonal phase (*T-phase*) with $(200)_T/(002)_T$ peaks, as shown in Fig. 1(c). The change in phase structure of the $(K_{0.41}Na_{0.59})(Nb_{1-x}Sb_x)O_3$ ceramics could be attributed to the fact that the ionic radius of the Sb^{3+} (0.76 Å) or Sb^{5+} (0.62 Å) ions were comparable to the radius of the Nb^{5+} atoms (0.78 Å) in the B-site and smaller than the radii of atoms such as K^+ (1.64 Å) and Na^+ (1.32 Å) that are present in the A-site, as shown in the ABO_3 model [5, 20, 22–24]. The results agreed well with previously reported results Jiang et al. [13] for $0.9(K_{0.5}Na_{0.5})(Nb_{1-x}Sb_x)O_3$-$0.1Bi(Ni_{2/3}Nb_{1/3})O_3$ and Nuraini et at. [14] for $(K_{0.5}Na_{0.5})NbO_3$ - $Ba_{0.8}Sr_{0.2}TiO_3$ and Gio et al. [15] for $(K_{0.48}Na_{0.48}Li_{0.04})(Nb_{0.95}Sb_{0.05})O_3$ - $Bi_{0.5}(Na_{0.82}K_{0.18})_{0.5}ZrO_3$.

Fig. 2 shows the microstructure of $(K_{0.41}Na_{0.59})(Nb_{1-x}Sb_x)O_3$ ceramics sintered at 1090°C for 2 h. As can be seen in Fig. 2, the average grain size of the ceramics ranged from 0.67 to 2.39 μm, and all ceramics possessed prominent grain boundaries. Generally speaking, with the addition of Sb modifies the microstructure of KNNS ceramics. As illustrated in Fig. 2(f), the grain size increased as the Sb concentration rose and peaked at 2.39 μm at x = 0.03. In the undoped KNN ceramic sample, the grain boundary is very clear, with many voids (Figure 2(a)), demonstrating low ceramic density (Fig. 3(a). The microstructure of the ceramic becomes denser, the grains are uniform, and the voids decrease with a ceramic pore size in the vessel of 1.76 μm (Figure 2(c). This is consistent with the increase in ceramic density with increasing Sb concentration. In other words, at x = 0.06, the best microstructure, the sample with the most tightly packed particles and the fewest

pISSN 1859-1388
eISSN 2615-9678

voids, this is the sample with the highest ceramic density (4.46 g/cm^3 (reaching 98.7% of the theoretical value) (Fig. 3(a)). In addition, with the increase of Sb concentration, the particle size decreased gradually and was smaller in the sample with x = 0.12 (Fig. 2(e)) with an average particle size of 0.81 μm. This is explained by the dissolution of Sb into the KNN lattice and forming a homogeneous solid solution. That means that Sb^{3+} ions (0.76 Å) or Sb^{5+} ions (0.62 Å) penetrate the KNN lattice and substitute for Nb^{5+} ions (0.78 Å) at position B due to similar radii [16]. It is this Sb doping that is responsible for the increase in ceramic density by creating the perfect microstructure of ceramic [17].

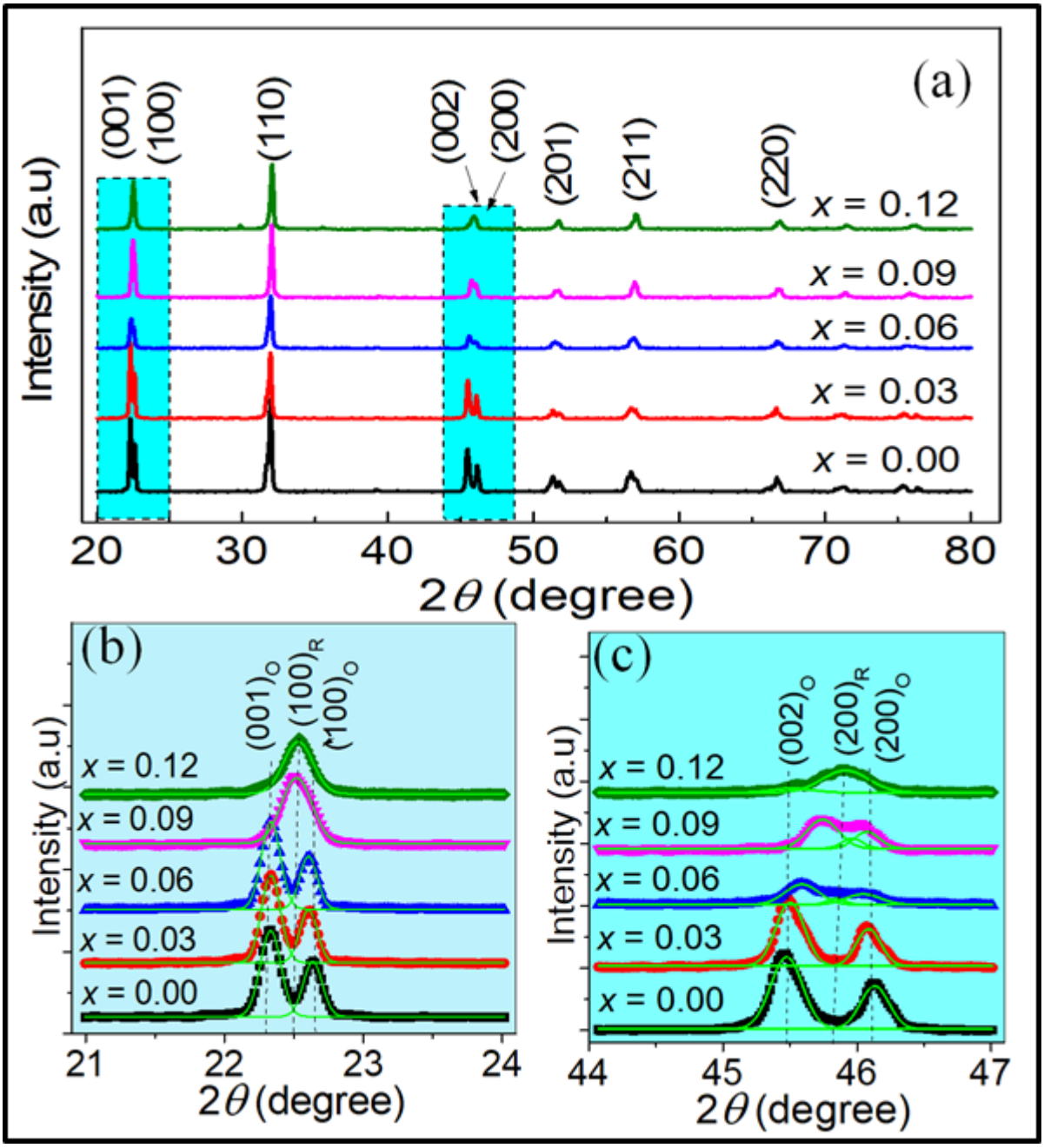

Fig. 1. XRD patterns recorded for $(K_{0.41}Na_{0.59})(Nb_{1-x}Sb_x)O_3$ ceramics under conditions of varying x

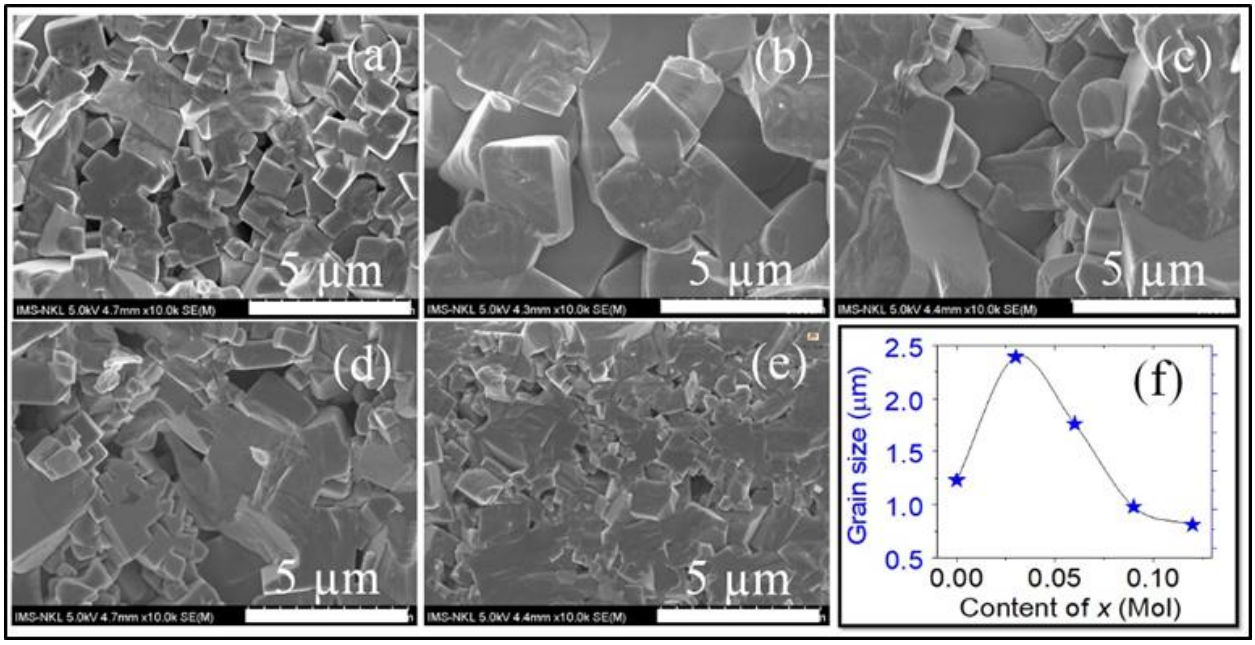

Fig. 2. Microstructures of $(K_{0.41}Na_{0.59})(Nb_{1-x}Sb_x)O_3$: a) x = 0,0; b) x = 0,03; c) x = 0,06; d) x = 0,09; e) x = 0,12; f) the average grain size of the semples

The dielectric loss (tanδ) and room temperature dielectric constant (ε) of Sb-doped KNN ceramics are measured at a frequency of 1 kHz, as shown in Fig.3. The dielectric constant ε increases with the x increases and reaches the highest value (ε = 945) at x = 0.06. However, when x > 0.06, the dielectric constant ε decreased. Conversely, when the x increases, the value of the dielectric loss tanδ decreases to the smallest value (tanδ = 0.15) at x = 0.06, then increases. These may be related to the density and microstructure of ceramics. According to the work of Ullah et al. [18], the high ceramic density, the large grain size, and the perfect microstructure are responsible for the increased dielectric properties.

The dielectric constant (ε) and dielectric loss (tanδ), which were measured at 1 kHz, are shown to depend on temperature in Fig. 4(a). As seen, all the $\varepsilon(T)$ curves of the ceramic samples have two obvious peaks: a peak at low temperature, which is the peak corresponding to the orthorhombic-tetragonal ferroelectric phase transition temperature ($T_{O\text{-}T}$), the second peak at higher temperatures, corresponding to the T_C temperature (called the ferroelectric-paraelectric phase transition) [19]. From Fig. 4(b) shows that the addition of Sb has a negligible influence on the $T_{O\text{-}T}$ and T_C phase transition temperatures of $(K_{0.41}Na_{0.59})(Nb_{1-x}Sb_x)O_3$ ceramics. Thus, Sb doping has a significant effect on the T_C and $T_{O\text{-}T}$ phase transition temperatures of ceramic $(K_{0.41}Na_{0.59})(Nb_{1-x}Sb_x)O_3$ and the values fluctuate in the range of 333–402 °C, and 150–250 °C, respectively. The T_C decreases but still maintains a high temperature when x = 0.06 (T_C = 371 °C) while the quite low $T_{O\text{-}T}$ of 157 °C. This result is consistent with the research results on the structure of ceramics and the similar with the result of [1-3] and Venet et al. [20]. Fig. 4(a) also shows that the peak of the sharp dielectric constant, indicating that the ceramics is a normal ferroelectric. The dielectric constant at T_C (ε_{max}) increases with the x increases and reaches the highest value (ε_{max} = 12031) at x = 0.06. However, when x > 0.06, the ε_{max} decreased (Fig. 4(b). This can be explained by the coexistence of the two *R-T* phases, resulting in the MPB effect, which eventually results in an increase in the mobility of the domains [21, 22].

pISSN 1859-1388
eISSN 2615-9678

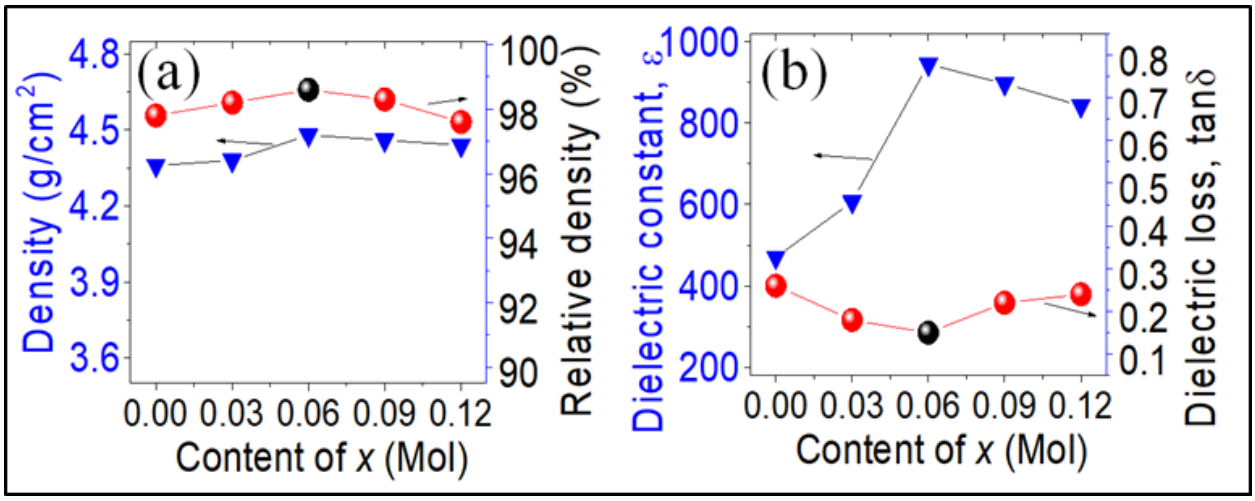

Fig. 3. (a) ceramic density; (b) dielectric constant and the dielectric loss of $(K_{0.41}Na_{0.59})(Nb_{1-x}Sb_x)O_3$

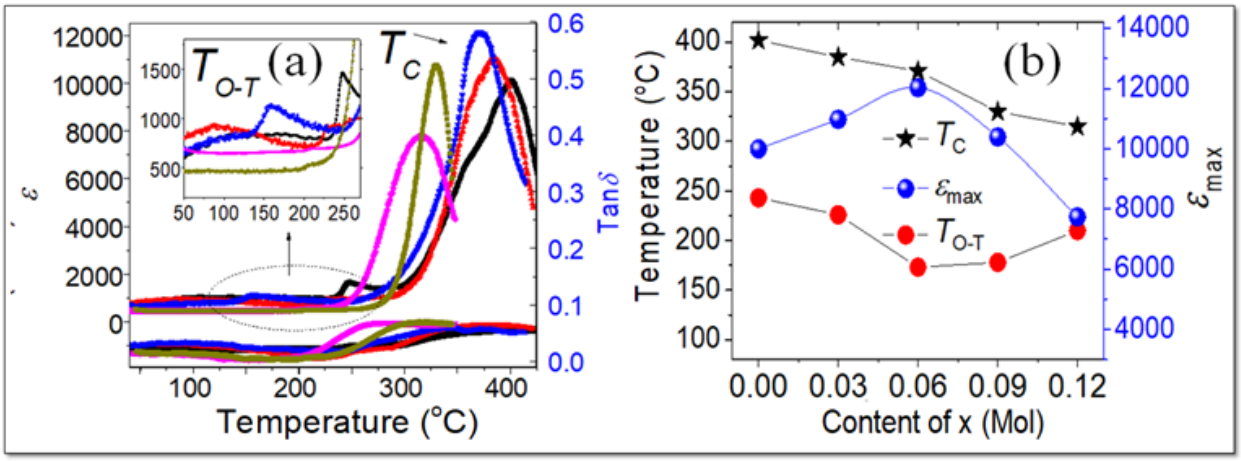

Fig. 4. Temperature-dependent dielectric constant and dielectric loss of $(K_{0.41}Na_{0.59})(Nb_{1-x}Sb_x)O_3$ at 1 kHz

Fig. 5(a) shows the shapes of *P-E* ferroelectric hysteresis loops measured at room temperature of the $(K_{0.41}Na_{0.59})(Nb_{1-x}Sb_x)O_3$ ceramic samples. As shown in figure 5(a-b), the Sb addition has an obvious influence on the ferroelectric properties of the ceramics. A round-shaped *P–E* hysteresis loop is obtained for the ceramics well-saturated *P–E* hysteresis loops are observed, showing good ferroelectric properties. The value of P_r increases with an increase in x and reaches the maximum value of 11.2 μC/cm^2 at x = 0.06, and then decreases. The E_c values decrease with an increase x and reach the minimum value of 6.7 kV/cm at x = 0.12, while E_c reaches the maximum value of 8.7 kV/cm at x = 0.06. The improvement in ferroelectric properties is attributed to the MPB effect, which results in the improvement in the orientation directions of the domains. It is thought that the perfect microstructure, small grain boundaries, and high ceramic density have improved the polarization of Sb-doped KNN ceramics. As previously discussed, the grain size and density increased with the increase in the Sb content, which helped improve the polarization of the ferroelectric ceramics. Similar findings have been published before [23], and they are consistent with the ceramics' studied dielectric characteristics.

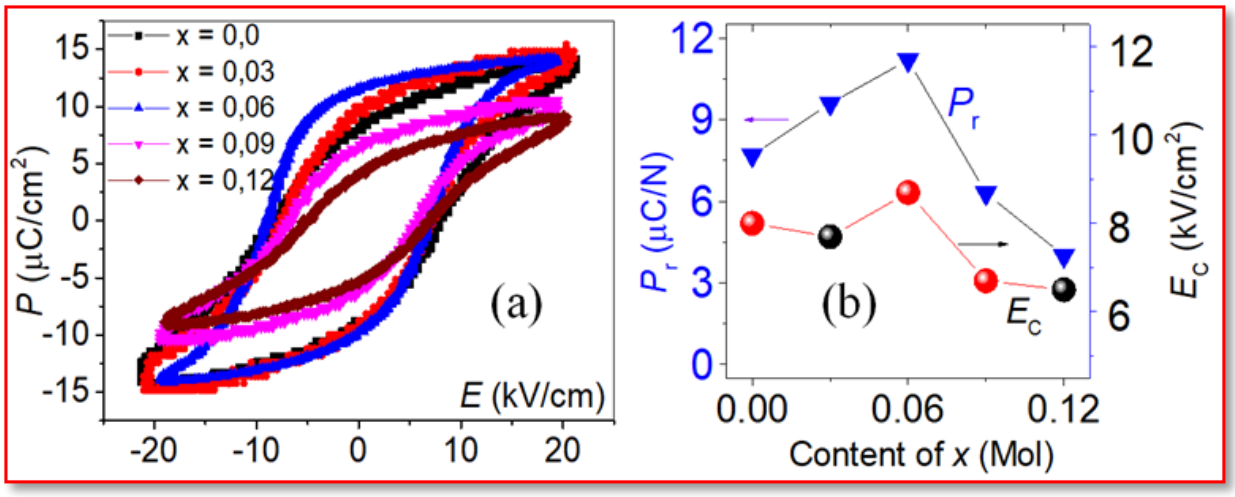

Fig. 5. Ferroelectric behavior of $(K_{0.41}Na_{0.59})(Nb_{1-x}Sb_x)O_3$ ceramics: (a) P–E hysteresis; (b) P_r and E_c values versus Sb contents

Table 1. Compilation of physical properties for the KNN-based ceramics with the other reported data

KNN-based ceramics	Density g/cm³	P_r (μC/cm²)	E_C (kv/cm)	T_C (ºC)	T_{O-T} (ºC)	ε	Ref.
$(Na_{0.59}K_{0.41})(Nb_{0.94}Sb_{0.06})O_3$	4.48	11.2	6.7	372	157	945	This work
$(K_{0.41}Na_{0.59})NbO_3$	4.36	11.6	6.7	404	238	470	[12]
$[Na_{0.5}K_{0.5}]_{0.95}(Li)_{0.05}(Sb)_{0.05}(Nb)_{0.95}O_3$	4.39	6.6	23.8	339	100	800	[24]
$K_{0.475}Na_{0.525})NbO_3$	4.31	10.5	11.1	425	217	450	[25]
$(Na_{1-x}K_x)NbO_3$	4.25	-	-	420	-	290	[26]

The KNN-based ceramics reported to date [12, 24-26] as listed in Table 1. Our results indicated that the $(Na_{0.59}K_{0.41})(Nb_{0.94}Sb_{0.06})O_3$ ceramics can be obtained at a lower sintering temperature (1090 ºC), while the dielectric and ferroelectric properties of the material ceramics are well-maintained.

4 Conclusions

The traditional mixed-oxide process was used to produce lead-free $(K_{0.41}Na_{0.59})(Nb_{1-x}Sb_x)O_3$ (KNNS) ceramics with x = 0.0, 0.03, 0.06, 0.09, and 0.12. The results show that all samples have pure perovskite phase and shifts from the orthorhombic structure to the mixed rhombohedral and tetragonal structure with an increase in the x value. With the x = 0.06, physical properties of $(Na_{0.59}K_{0.41})(Nb_{0.94}Sb_{0.06})O_3$ ceramics are best: the density of 4.48 g/cm³; the dielectric constant (ε) *of* 945; the dielectric loss (tanδ) of 0.15; the remanent polarization (P_r) of 11.2 μC/cm², and the reactance field (E_c) of 8.7 kV/cm, and the phase transition temperatures (T_c) of 372 °C, (T_{O-T}) of 157 °C.

Acknowledgments:

This research was funded by Ministry of Education and Training under grant number B2022-ĐHH-06.

References

1. Cheng X, Wu J, Wang X, Zhang B, Zhu J, Xiao D, et al. Giant d_{33} in (K,Na)(Nb,Sb)O_3-(Bi, Na, K, Li)ZrO_3

pISSN 1859-1388
eISSN 2615-9678

based lead-free piezoelectrics with high T_c. Applied Physics Letters. 2013;103(5).

2. Dinh Tung Luan N, Vuong LD, Van Chuong T, Truong Tho N. Structure and physical properties of PZT-PMnN-PSN ceramics near the morphological phase boundary. Advances in Materials Science and Engineering. 2014;2014:821404.
3. Vuong LD, Gio PD, Quang NDV, Hieu TD, Nam TP. Development of $0.8Pb(Zr_{0.48}Ti_{0.52})O_3$–$0.2Pb[(Zn_{1/3}Nb_{2/3})_{0.625}(M_{1/3}Nb_{2/3})_{0.375}]O_3$ Ceramics for High-Intensity Ultrasound Applications. Journal of Electronic Materials. 2018;47(10):5944-51.
4. Gio PD, Viet HQ, Vuong LD. Low-temperature sintering of 0.96 $(K_{0.5}Na_{0.5})NbO_3$-0.04 $LiNbO_3$ lead-free piezoelectric ceramics modified with CuO. International Journal of Materials Research. 2018;109(11):1071-1076.
5. Vuong LD, Gio PD. Enhancement in dielectric, ferroelectric, and piezoelectric properties of $BaTiO_3$-modified $Bi_{0.5}(Na_{0.4}K_{0.1})TiO_3$ lead-free ceramics. Journal of Alloys and Compounds. 2020;817:152790.
6. Vuong LD, Gio PD. Effect of Li_2CO_3 addition on the sintering behavior and physical properties of PZT-PZN-PMnN ceramics. International Journal of Materials Science and Applications. 2013;2(3):89-93.
7. Tuan DA, Vuong LD, Tung VT, Tuan NN, Duong NT. Dielectric and ferroelectric characteristics of doped BZT-BCT ceramics sintered at low temperature. Journal of Ceramic Processing Research. 2018;19(1):32-36.
8. Wongsaenmai S, Ananta S, Yimnirun R. Effect of Li addition on phase formation behavior and electrical properties of $(K_{0.5}Na_{0.5})NbO_3$ lead free ceramics. Ceramics International. 2012;38(1):147-52.
9. Wang K, Li J-F, Liu N. Piezoelectric properties of low-temperature sintered Li-modified (Na, K) NbO_3 lead-free ceramics. Applied Physics Letters. 2008;93(9).
10. Li P, Zhai J, Shen B, Zhang S, Li X, Zhu F, et al. Ultrahigh piezoelectric properties in textured (K, Na) NbO_3-based lead-free ceramics. Advanced Materials. 2018;30(8):1705171.
11. Gio PD, Vuong LD, Tu LTU. Enhanced piezoelectric and energy storage performance of $0.96(K_{0.48}Na_{0.48}Li_{0.04})(Nb_{0.95}Sb_{0.05})O_3$–$0.04Bi_{0.5}(Na_{0.82}K_{0.18})_{0.5}ZrO_3$ ceramics using two-step sintering method. Journal of Materials Science: Materials in Electronics. 2021;32(10):13738-47.
12. Tu LTU, Gio PD. Systematic study of the influence of the K/Na ratio on the structure, microstructure, and electrical properties of $(K_xNa_{1-x})NbO_3$ lead-free ceramics. Journal of Materials Science: Materials in Electronics. 2023;34(3):217.
13. Jiang J, Chen S, Zhao C, Wu X, Gao M, Lin T, et al. Effects of Sb Doping on Electrical Conductivity Properties in Fine-Grain KNN-Based Ferroelectric Ceramics. Crystals. 2022;12(9):1311.
14. Nuraini U, Triyuliana NA, Mashuri M, Kidkhunthod P, Suasmoro S. Local distortion determination of the $(1-x)(K_{0.5}Na_{0.5})NbO_3 - x\,(Ba_{0.8}Sr_{0.2})TiO_3$ system and their influence on the electrical properties. Journal of Materials Science: Materials in Electronics. 2018;29(2):1139-45.
15. Gio PD, Vuong LD, ThanhTung V. Phase transition behavior and electrical properties of lead-free (1-x)KNLNS-xBNKZ piezoelectric ceramics. Journal of Electroceramics. 2021;46(3):107-14.
16. Vuong LD, Truong-Tho N. Effect of ZnO Nanoparticles on the Sintering Behavior and Physical Properties of $Bi_{0.5}(Na_{0.8}K_{0.2})_{0.5}TiO_3$ Lead-Free Ceramics. Journal of Electronic Materials. 2017;46(11):6395-402.
17. Vuong LD, Quang DA, Tung VT, Chuc NH, Trac NN. Synthesis of textured $Bi_{0.5}(Na_{0.8}K_{0.2})_{0.5}TiO_3$–$Ba_{0.844}Ca_{0.156}(Zr_{0.096}Ti_{0.904})O_3$ lead-free ceramics for improving their electrical and energy storage properties. Journal of Materials Science: Materials in Electronics. 2020;31(20):18056-69.
18. Ullah A, Ahn CW, Hussain A, Kim IW. The effects of sintering temperatures on dielectric, ferroelectric and electric field-induced strain of lead-free Bi0. 5 $(Na_{0.78}K_{0.22})_{0.5}TiO_3$ piezoelectric ceramics synthesized by the sol–gel technique. Current Applied Physics. 2010;10(6):1367-7.
19. Wang Y, Lu Y, Wu M, Wang D, Li Y, Wang Y. Phase Structure and Enhanced Piezoelectric Properties of Lead-Free Ceramics $(1-x)(K_{0.48}Na_{0.52})NbO_3$–$(x/5.15)K_{2.9}Li_{1.95}Nb_{5.15}O_{15.3}$ with High Curie Temperature. International Journal of Applied Ceramic Technology. 2012;9(1):221-7.
20. Venet M, Santa-Rosa W, da Silva PS, M'Peko J-C, Ramos P, Amorín H, et al. Selection and Optimization of a $K_{0.5}Na_{0.5}NbO_3$-Based Material for Environmentally-Friendly Magnetoelectric Composites. Materials. 2020;13(3):731.
21. Vuong LD. Densification behavior and electrical properties of the PZT-PZMnN-based ceramics

prepared by two-step sintering. Journal of Materials Science: Materials in Electronics. 2022;33(9):6710-21.

22. Quang DA, Vuong LD. Enhanced piezoelectric properties of Fe_2O_3 and Li_2CO_3 co-doped $Pb[(Zr_{0.48}Ti_{0.52})_{0.8}(Zn_{1/3}Nb_{2/3})_{0.125}(Mn_{1/3}Nb_{2/3})_{0.075}]O_3$ ceramics for ultrasound transducer applications. Journal of Science: Advanced Materials and Devices. 2022;7(2):100436.

23. Wang K, Zhu X, Zhang Y, Zhu J. Low temperature synthesis and enhanced electrical properties of PZN–PNN–PZT piezoelectric ceramics with the addition of Li_2CO_3. Journal of Materials Science: Materials in Electronics. 2017;28(20):15512-8.

24. Rani R, Sharma S, Rai R, Kholkin A. Doping effects of Li–Sb content on the structure and electrical properties of $[(Na_{0.5}K_{0.5})_{1-x}(Li)_x(Sb)_x(Nb)_{1-x}O_3]$ lead-free piezoelectric ceramics. Materials Research Bulletin. 2012;47(2):381-6.

25. Yin J, Wu J, Wang H. Composition dependence of electrical properties in $(1-x)KNbO_3–xNaNbO_3$ lead-free ceramics. Journal of Materials Science: Materials in Electronics. 2017;28(6):4828-38.

26. Egerton L, Dillon DM. Piezoelectric and Dielectric Properties of Ceramics in the System Potassium—Sodium Niobate. 1959;42(9):438-42.